bioresources.cnr.ncsu.edu

Flexural Performance and Failure Mode of Wood-Based Sandwich Structure Plate Members

Donxia Yang ![ORCID],[a] Lihua Guo,[a,*] and Changsheng Fan ![ORCID],[b]

Pyramid-type and lattice-type sandwich structure plate members were designed and fabricated using oriented strand board as the panel and larch finger-joined lumber as the core material, while glass fiber was used as the panel reinforcing material. The mechanical properties of the four types of sandwich structure plate members were tested by four-point bending test. The test results showed that the damage forms of the plate members were mainly the debonding between the core and the panel and the bending failure of the core. It can be concluded from the mechanical properties of plate members with sandwich structure that the transfer path and efficiency between the panel and the core layer of a sandwich structure plate members have a decisive influence on the flexural performance of the specimen. The core configuration determines the relative stiffness ratio between the panel and the core. This study was able to provide reliable experimental data and theoretical support for the application of wood-based sandwich structure plate members in prefabricated temporary buildings, landscape timber structures, and other fields, in order to promote their optimized design and wide application.

*Contact information: a: Key Laboratory of Heilongjiang Underground Engineering Technology, Harbin University, Harbin 150086 China; b: Laboratory of Bio-Based Material Science & Technology of Ministry of Education, College of Computer and Control Engineering, Northeast Forestry University, Harbin 150040 China; *Corresponding author: changshengfan @nefu.edu.cn*

INTRODUCTION

Wood is a very rich and versatile material that has been the primary energy source, tool, building foundation, insulation material, and furniture for humanity for thousands of years (Lukawski *et al.* 2023). To get the most out of the wood, it needs to be protected, modified, multi-layer bonded, and cross-sectionally optimized to ensure the structure has adequate stiffness and strength. In order to achieve a wood structure with higher strength and lighter weight, the current common method is to first improve the existing wood varieties, second is the sandwich structure, and third is to design a cavity or skeleton with a unique shape and connected with the panel to reduce the weight of the wood core as much as possible (Tian *et al.* 2024).

For the third design, there are currently many commercially available high-efficiency engineered wood products available for construction worldwide. For example, prefabricated wooden I-joists are popular as structural beams in residential building flooring and roof applications (De Santis *et al.* 2023). They are characterized by their light weight, high strength and stiffness, dimensional stability, and low cost compared to traditional wood beams (Jiloul *et al.* 2024). For decades, oriented strand board (OSB) has been the most widely used core material in the manufacture of I-joists. The preference for

OSB is due to its reasonable cost and satisfactory stiffness and strength compared to other wood-based structural panels (Ardalany *et al.* 2013). Wood I-joists with OSB webs and either solid-sawn or laminated flanges are widely used in construction, their behavior and design are well understood, and they are efficient to manufacture (Chen *et al.* 2021). Although the wood I-joist and their forms exhibit mechanical and structural properties, this structural element hides some structural defects that must be addressed. The main failure modes of wood I- joist during load-bearing include interlayer shear failure of the web plate, flange failure, and web plate instability failure. Wood I-joists are susceptible to failure before reaching their full load capacity, as the thin web structure tends to deform before the critical buckling load is reached. This buckling instability phenomenon is considered a limitation of the I-joist and results in a decrease in its structural capacity. Many strengthening mechanisms and methods have been developed to improve the behavior of I-joists and increase their stability and ability to resist buckling. Modifying the materials or geometric shape of the web, or even installing stiffeners, is one of the most effective solutions against buckling (Dubina *et al.* 2015; Aydin *et al.* 2016; Jiao *et al.* 2017).

The research in this article is mainly based on the second method, which applies wooden materials to sandwich structures to form wood-based sandwich structural materials. The sandwich structure is composed of two relatively thin parallel panels and a relatively thick lightweight core layer bonded together. The panels mainly bear bending and in-plane loads, while the core layer mainly bears transverse shear forces transmitted from the panels, while supporting the panels and preventing local buckling. According to whether the core topology is regular or not, the sandwich structure can be divided into two categories: disordered foam sandwich structure and porous sandwich structure with orderly cell cycle (Du *et al.* 2022).

The sandwich structure has the characteristics of light weight, high strength, high energy absorption, and high energy dissipation (Smardzewski *et al.* 2022). The structure has been widely used in aerospace (Juliette *et al.* 2023; Pierre *et al*. 2023), vehicle engineering (Zulueta *et al.* 2022), and prefabricated building assemblies (Almutairi *et al.* 2023). Researchers are committed to improving the performance of sandwich structures and improving them by optimizing the type of core layer, changing the core layer structure, and adding filling materials.

Due to the durability and wide applicability of metal composite materials, sandwich structures made of metal composite materials have become the preferred material across multiple industry sectors (Amir *et al.* 2021, 2023; Singh *et al.* 2024). Faidzi *et al.* (2021) introduced the achievements and trends of sandwich panels in the past 50 years, and re-evaluated the current core material design, materials, and failure mechanisms of metal-based sandwich panels. Han *et al*. (2017) conducted a literature review on the performance of hybrid grid sandwich structural panels in enhancing structural load-bearing capacity, energy absorption, and sound absorption. The automotive manufacturing industry is one of the largest users of metal-based sandwich panels, using sandwich panel technology such as replacing bonded integral panels with several types of panels made of different materials. Hara and Ozgen (2016) investigated the application of sandwich materials in automotive body panels. To enhance the performance of metal sandwich composite panels, Kamble *et al.* (2021) proposed woven spacer fabric to strengthen the sandwich structure, giving it higher shear stiffness and out of plane compression strength. The cross-linking structure of the WSF has been used to solve the delamination problem of traditional sandwich composite materials (Wang *et al.* 2022). The commonly used materials in sandwich structures include aluminum alloys, titanium alloys, fiber-reinforced polymers,

magnesium, shape memory alloys, high-strength steel, ceramic matrix composites (CMC), and wood composites (Blanco *et al.* 2021; Hassan and Saeed 2024).

Wood-based sandwich structures have been lagging behind the development of many industrial sandwich structures (Kawasaki *et al.* 2006). Regarding the study of wood-based sandwich structures, Pelinski and Smardzewski (2020) and Smardzewski *et al.* (2022) investigated the flexural behavior of wood-based sandwich beams. The panels of the sandwich beams were made of plywood, and the core materials were high-density fiberboard, cardboard, and epoxy resin to create sandwich beams with an auxetic cellular core. The stiffness, strength, and energy absorption capacity of sandwich beams can be evaluated through three-point flexural tests. The research results indicate that sandwich structure beams with auxetic cellular cores can bear high deflection expansion core beams (Pelinski and Smardzewski (2020); Smardzewski *et al.* 2022). Zheng *et al.* (2021) studied the shear performance and failure mode of short beams in a wood-based X-shaped lattice sandwich structure. Oriented strand board (OSB) was used as the panel in the study, with an X-shaped lattice structure as the core layer and birch wood as the material. Studies have shown that the main failure mode of sandwich beams is the wrinkling and crushing of the panels (Zheng *et al.* 2021). Hao *et al.* (2018) studied the use of medium density fiber board and plywood as panels and made a Taiji hexagonal cell structure from kraft paper as the core layer. The static flexural mechanical properties of this lightweight composite sandwich panel were studied through three-point flexural tests, and the shear strength of the Taiji honeycomb structure beam was 3.44 times that of the ordinary hexagonal honeycomb structure (Hao *et al.* 2018).

Mohammadabadi *et al.* (2023) studied the use of wooden molds to manufacture corrugated sandwich panels. The panels were made of 4-mm thick southern yellow pine veneers, and the cores material were made of 0.68 mm thin red-oak veneers to produce corrugated panels. Cold forming technology was used to manufacture wood-based sandwich panels. The four-point flexural test was applied to evaluate its structural performance. The experimental research results show that compared with flat plates made of the same stacking of veneers, the flexural stiffness of the sandwich panel increased by 272% (Mohammadabadi *et al.* 2023). Li *et al.* (2016) studied the static and fatigue flexural properties of wood fiber based triaxial engineering sandwich composite panels in four-point flexural tests. In static flexural tests, structural failure occurs at the surface layer of the pure flexural zone, while in fatigue flexural tests, structural failure occurs at the boundary between the surface layer and the core layer of the shear zone (Li *et al.* 2016).

For biomass-based building materials, Wang *et al.* (2024) studied the structural forms of triangular, square, and Kagome lattice structures as the core layer. They used interlocking and segmentation methods to produce bamboo laminated sandwich panels and conducted four-point flexural tests on them. The flexural test shows that the triangular lattice sandwich panel has the best load-bearing capacity and specific strength (Wang *et al.* 2024). The wood-based honeycomb sandwich beam studied by scholars such as Slonina *et al.* (2023) consists of a 3.0-mm thick particleboard panel, with a hexagonal structure made of impregnated modified starch paper as the core layer. After the three-point flexural test, it was verified that the thickness of the facing determines the strength and stiffness of the honeycomb panels, that the impregnation of the core with modified starch causes a slight deterioration in the strength and stiffness of the beams, and that the dominant type of beam failure is shear damage to the thin-walled core (Slonina *et al.* 2023).

Through comprehensive analysis of the existing research, it is found that most studies have been conducted on metal matrix composite sandwich structures, and there has

been relatively little research on the flexural performance of wood-based composite sandwich structure plate members. This paper mainly studied the bending behavior and failure mode of pyramid and grid type wood-based sandwich plate members. In this study, general woodworking equipment such as panel saws, drill press, and milling machines were used for the processing of the specimens of the wooden sandwich structure plate members. Using numerical simulation and experimental methods, the goal was to analyze the failure mechanism and mechanical properties of wooden pyramid type sandwich structure plate members and grid type sandwich structure plate members under four point bending loads. This study can provide reliable experimental data and theoretical support for the application of wood-based sandwich structure plate members in prefabricated temporary buildings, landscape timber structures, and other fields, in order to promote their optimized design and wide application.

EXPERIMENTAL

To investigate the mechanical properties of wood-based sandwich structure plate members under four-point flexural loads, this study designed two different core layer structures: one was a pyramid shaped core layer, and the other was a grid shaped core layer. The tests were performed according to ASTM C393 M-06 (2006), ASTM D7249 (2016), and ASTM D7250M-16 (2016).

Before conducting the experimental tests on wooden core sandwich structures plate members, flat compression tests were performed on pyramidal cellular elements and interlocking grillage cellular elements. Larch, Birch, WPC, OSB, and Plywood materials were used to fabricate pyramid typed cells of Larch +Birch, WPC +Birch, and OSB +Birch, as well as interlocking grid typed cells of Larch +Larch, Plywood +Larch, and OSB +Larch. The flat compression performance experiments were conducted on these structural cells, and the results showed that the cells composed of OSB +Larch had better flat compression performance (Yang *et al.*2022). Therefore, in terms of material selection for this experiment, larch was used for the core layer and OSB was used for the panel. Through this design, the aim is to deeply analyze the influence of different core structures on the mechanical properties of wooden sandwich plate members. These two materials have similar densities and coefficients of thermal expansion, which helps to reduce structural deformation and internal stress caused by temperature changes (Huang *et al.* 2014). At the same time, they can make the weight distribution of the entire sandwich structure more balanced, reduce local stress concentration caused by differences in material density, and improve the overall stability of the structure (Feng *et al.* 2008). The goal is to reduce the interfering factors introduced during the testing process due to differences in the physical properties of wood itself, thereby ensuring the accuracy and reliability of the test results.

Glass fiber reinforced composite materials (GFRP) were used to reinforce the face panel, and face panel reinforced specimens of the sandwich structure plate members were prepared. Through comparative tests of these four specimens, the key factors affecting the mechanical and bending properties of the sandwich structure plate members were identified. Provide a solid theoretical foundation and experimental basis for subsequent structural optimization and performance improvement.

Mechanical Properties of Raw Materials

The face panel material of the specimens of the sandwich structure plate members is OSB. The longitudinal direction of OSB is the directional arrangement of the surface particles of oriented strand board along the length of the board. The transverse and longitudinal directions of OSB are perpendicular, and its mechanical properties are lower than those of the main axis (Yang *et al.* 2021). The OSB was imported from Germany, with an environmental grade of E0, and purchased from Dongfang Port International Timber Co., Ltd. The core material of the specimens of the sandwich structure plate members was selected as larch. Larch finger jointed lumber was purchased from Dafa Wood Industry in Harbin, China. The tooth length of the finger joint lumber was 12 mm. The finger joint frequency was 1.5 per meter. The panel surface of the specimens of the sandwich structure plate members was bonded with a layer of GFRP adhesive, thus forming face panel reinforced specimens of the sandwich structure plate members. GFRP (Li *et al.* 2024) material was E-Glass woven rovings. The fiber weaving angle was (0.90 °), and the area density of single-layer fiber cloth was 410 g/m^2. GFRP uses unsaturated polyester resin produced by Nantong Chemical and Light Industry Co., Ltd. as the matrix material. Huiyuan Shi's research on the mechanical properties of GFRP shows that the fiber braiding angle of the material has little effect on its mechanical properties (Shi *et al.* 2018). The adhesive used was epoxy resin, which was purchased from the Institute of Petroleum Chemistry, Heilongjiang Academy of Sciences, Harbin, China.

To investigate the specific effects of different core layer configurations on the mechanical properties and bending resistance of sandwich structure plate members, two types of sandwich structure plate members with different core layer configurations were prepared. The middle part of the pyramid sandwich structure beam is composed of round bar tenons, while the middle part of the grid sandwich structure beam was composed of multiple rib plates. Mechanical properties of test raw materials are listed in Table 1.

Table 1. Mechanical Properties of Raw Materials

Material	Shaving Direction	ρ (g/cm³)	MOE (GPa) Compressive	MOR (MPa) Compressive
OSB	Horizontal	0.61	3.52	22.37
	Longitudinal		3.05	20.23
Larch finger-jointed lumber	Longitudinal	0.51	26.68	50.30
GFRP	-	-	19.57	158.11

Prefabricated Wood-Based Pyramid Sandwich Structure Plate members

The prefabricated wood-based pyramid sandwich structural plate members is composed of pyramid structure unit cell. The wood-based pyramid sandwich structure specimen of the plate members is shown in Fig. 1. The flat compression mechanical properties of the cellular structure shown in Fig. 1 (b) and (c) have been studied (Yang 2022). The structural dimensions of the cell in the pyramid type wooden sandwich structure plate members are shown in Table 2. The specimens are connected by three pyramidal cells to form a pyramidal sandwich structural plate members. The preparation of pyramid sandwich structure plate members involves assembling multiple cells into sandwich structure plate members using assembly strips. First, the upper and lower panel sides of the pyramid sandwich structure cell were slotted. A bench drill was used to drill holes in the upper and lower panels. Then, the adhesive was applied evenly to the surface of the hole, inserting the core into the hole to fix it by bonding. Finally, adhesive was applied evenly

to the grooves on the sides of the upper and lower panels of the pyramid structure cells. Multiple cells were connected with assembly strips to form a sandwich structure plate members. To improve the adhesion between the specimens, two panels were placed on the prepared specimens and kept at room temperature for 3 days to ensure the reliability of the experimental results. Five specimens were prepared.
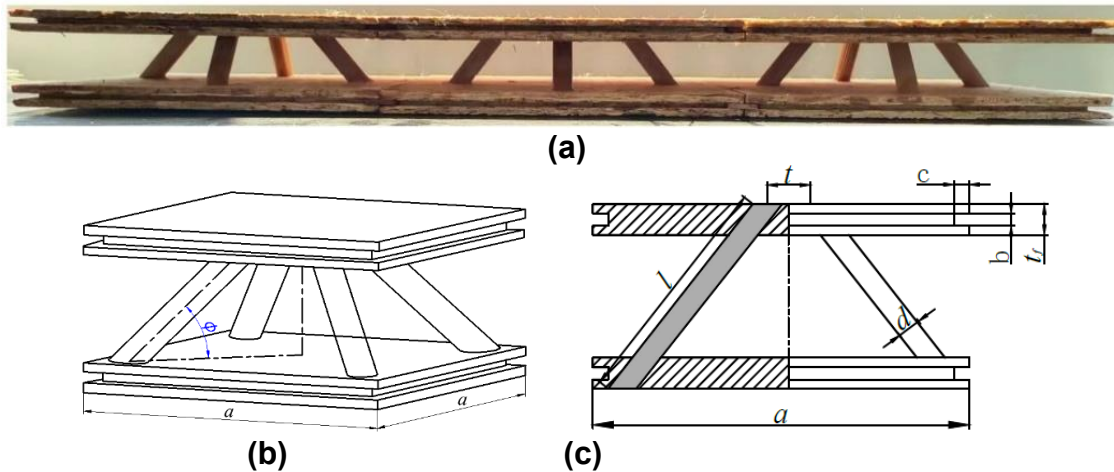

(a)

(b)　　　　　　　**(c)**

Fig. 1. Specimen of wood-based pyramid sandwich structure plate member. (a) specimen the of pyramid type sandwich structure plate members; (b) axonometric drawing of pyramid type structure cell; (c) section view of pyramid type structure cell

Table 2. Structural Parameters of the Pyramid Sandwich Structure Cell (unit: mm)

Type	a	b	c	d	tf	t	φ
Pyramid	200	3	3	12	12	46	52°

　　　　The upper and lower panels of the pyramid sandwich structure plate members cell were square. The middle part of the panel side was slotted. Assembly strips were placed in the slots and fixed with adhesive, which connected the cells to form large-sized plate members to meet engineering needs. The middle part was a round bar tenon with a 52° inclination angle to the bottom surface. The stable stacking angle of the powder was 52°; therefore, the angle between the round tenon and the bottom surface was defined as 52°.

　　　　As shown in Fig. 1, the core of sandwich structure plate members is the cell. By using tenon and groove technology, multiple cells can be combined into various structural forms and large specimens. These specimens can form various forms such as hollow slabs, beams, columns, *etc*., which is in line with the current actively promoted concept of prefabricated timber structures (Jingxing *et al.* 2018; Mohammadabadi *et al.* 2023). According to the needs of practical applications, the size of the cell can be adjusted, thereby further expanding the breadth of its application fields.

Wood-based Grid Sandwich Structure Plate Members

　　　　To study the influence of different sandwich structure forms on the flexural performance of sandwich plate members, under the same conditions of panel material and core material, grid sandwich structure plate members were simultaneously prepared, and the specimen is shown in Fig. 2. The structural dimensions of the cell in the grid type

wooden sandwich structure plate members are shown in Table 3. The upper and lower panels of the grid sandwich structure plate members had grooves with the same thickness as the rib plate. The adhesive was evenly applied to the groove surface, and the rib plate was inserted into the groove and bonded and fixed. To improve the adhesion between the test specimens, two panels were placed on the prepared test specimens and kept at room temperature for 3 days to ensure the reliability of the experimental results. Five specimens were prepared for each type.

　　　　　Compared with pyramid structure, this kind of structure has the advantages of convenient processing and production of specimens and higher positioning accuracy of cores. The mass of the specimen of the same size is larger than that of the pyramidal sandwich plate members due to the large number of rib plates of the grid sandwich plate members.
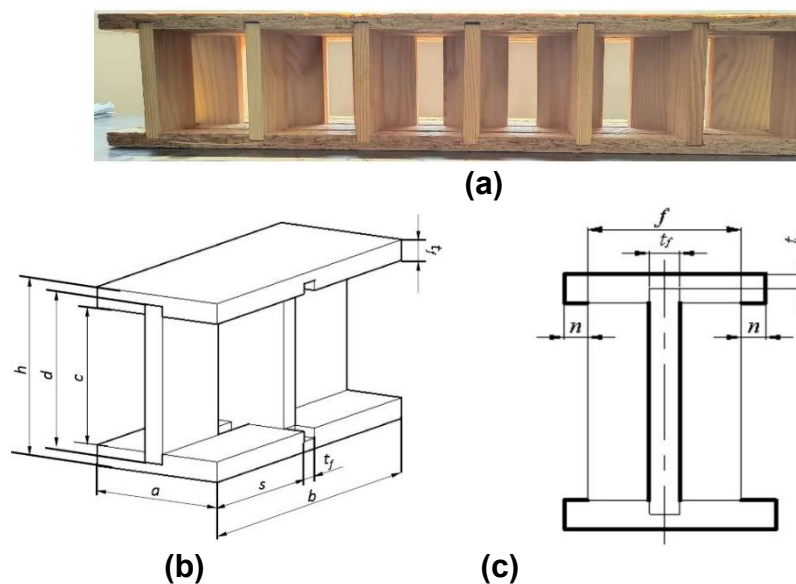

(a)

(b)　　　　　　　　　　　　　　**(c)**

Fig. 2. Specimen of wood-based grid sandwich structure plate members. (a) specimen the of grid type sandwich structure plate members; (b) axonometric drawing of grid type structure cell; (c) section view of grid type structure cell

Table 3. Structural Parameters of the Grid Sandwich Structure Cell (unit: mm)

Type	a	b	c	d	h	t_f	S	f	n	t
Grid	80	200	82	94	106	12	94	60	10	6

Panel Reinforcement Specimen

　　　　　GFRP has the characteristics of high specific modulus, low cost, corrosion resistance, and overall semitransparent appearance, which can effectively suppress the development of cracks in wooden structures (Huiyuan *et al.* 2018; Yang *et al.* 2022). In this experiment, 02 # glass fiber grid cloth was selected as the reinforcing material for the face panel. This material has fine texture, light weight, and good adhesion performance, making it suitable for application on the surface of the panel. The upper and lower panels of the test specimen need to be covered with GFRP, with a size of 200×600 mm^2. The GFRP material was bonded to the panel surface of the specimen with epoxy resin to form a panel-reinforced specimen. The panel reinforced specimen is shown in Fig. 3. The

bending behavior of wood-based sandwich structure plate members was studied through bending tests, providing reference for the design and application of wood-based sandwich plate members.
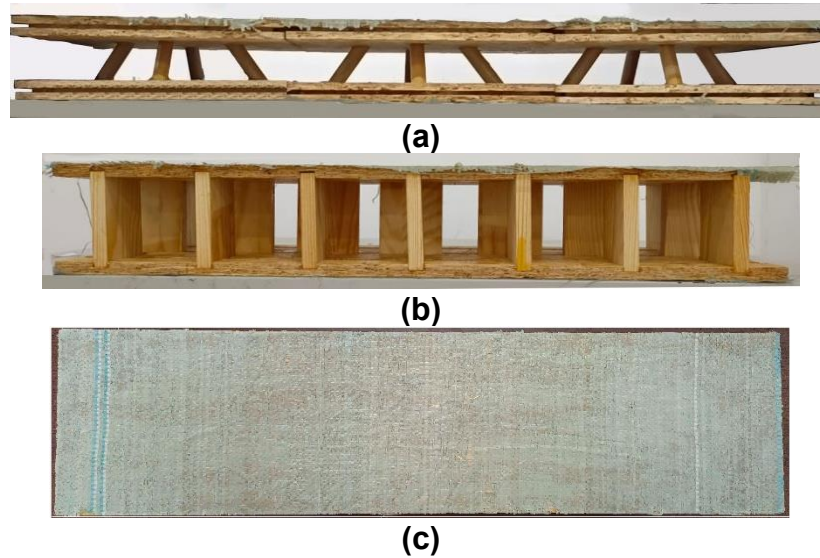

Fig. 3. Specimens of panel reinforced sandwich structure plate member. (a) Pyramid sandwich structure plate member; (b) Grid sandwich structure plate member; (c) Vertical view of the specimen

According to ASTM D7249 (2016) and ASTM D7250 (2016), four-point flexural tests were conducted on wood-based sandwich structural plate members at room temperature. This testing and loading method can maximize the flexural stress of the panel material while minimizing the shear stress within the core material.

The sample was tested using a microcomputer-controlled electronic universal testing machine. The model of the testing machine was WDW-50, purchased from Changchun Kexin Technology Co., Ltd. in China. There was a 500 kN weighing sensor on the WDW-50 testing machine. The sensor model was TDZ-1E-43, which is a linear variable differential transformer (LVDT); LVDT can be used to measure the maximum bending deflection at the mid span of a specimen. The loading rate of the experiment was 1 mm/min, and the experimental temperature was 20 ± 2 °C.

The length of the specimen was 600 mm, the width was 200 mm, the span of the top loading point was 100 mm, and the thickness of the plate was 12 mm. The height of the core layer is denoted as c. The height of the specimen is denoted as d. The span between two points of the specimen is denoted as L. The cylindrical loading roller with a pressure head had a diameter of 30 mm.

The specimens of the sandwich structure plate members used in this experiment had different core structures, panel and core materials, and their bending performance will be affected by various factors. Compared with the three-point bending test, the four point bending test can make the bending stress distribution on the specimen relatively more uniform in the loading method, reducing the edge effect near the loading point, and at the same time, the four point bending test is closer to the actual working conditions, which can more accurately reflect the overall bending performance of the specimen.

As shown in Fig. 4, the flexural resistance performance of the structure can be obtained from the load deflection curve. The prefabricated pyramid sandwich structure plate members is referred to as an I-type specimen, and the face panel reinforced prefabricated pyramid sandwich structure plate members is referred to as an RI-type specimen. The grid sandwich structure plate members is referred to as an II-type specimen, and the face panel reinforced grid sandwich structure plate members is referred to as an RII-type specimen. The specific dimensions of the specimen are shown in Table 4. $\overline{\rho}$ in Table 4 is the apparent density of the specimen structure. The apparent density is the ratio of the sample mass to its apparent volume. When calculating in this article, the volume of the specimen measured is directly recorded as the apparent volume of the specimen.
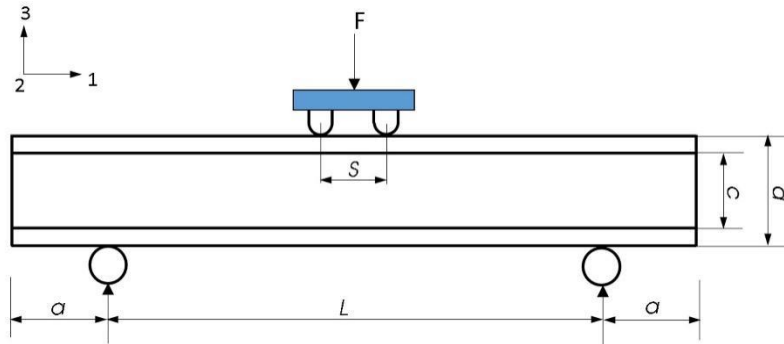

Fig. 4. Four-point flexural schematic diagram of sandwich structural plate members

Table 4. The Structural Parameters of the Specimen (Unit:mm)

Type	$\overline{\rho}$ (g/ cm³)	L+2a	L	c	d	s	B
I	0.27	600	480	28	52	100	200
RI	0.27	600	480	28	54	100	200
II	0.19	600	370	82	106	100	200
RII	0.18	600	370	82	108	100	200

The Equivalent Parameter of Sandwich Structure Plate Members

Flexural stiffness is an important parameter that describes the ability of a structure to resist flexural deformation when subjected to external forces. It can reflect multiple properties such as structural stability, durability, and material utilization. Wood-based sandwich structures with high flexural stiffness can maintain small flexural deformation when subjected to external forces, thereby ensuring the overall stability of the structure.

Since there is currently no formula for calculating the bending stiffness of sandwich panel components, this article adopts the proposal for the bending stiffness of sandwich beams from Allen (1969),

$$D = D_f + D_0 + D_c \tag{1}$$

where D is the flexural stiffness of the sandwich structure (N·mm²), and D_f is the flexural stiffness of the panel when bending its own axis(N·mm²).

$$D_f = E_f \frac{bt_f^3}{12} \tag{2}$$

In Eq. 2, D_0 is the flexural stiffness of the upper and lower panels when bending relative to the central axis of the sandwich structure beam (N·mm²).

$$D_0 = 2E_f \left(\frac{bt_f^3}{12} + Aa^2 \right) \tag{3}$$

In Eq. 3, A is the cross-sectional area of the panel,

$$A = b \cdot t_f \tag{4}$$

where a is the parallel axis, which is the distance from the center of the panel to the center of the sandwich structure beam,

$$a = \left(\frac{t_f + c}{2} \right) \tag{5}$$

and where D_c is the flexural stiffness of the core material when bending its own central axis ($N \cdot mm^2$).

$$D_c = E_c \frac{bc^3}{12} \tag{6}$$

In Eq. 6, E_f is the elastic modulus of the panel (MPa), E_c is the elastic modulus of the core material (MPa), t_f is the thickness of the panel (mm), b is the width of the specimen (mm), c is the thickness of the core layer (mm), and d is the height of the specimen (mm).

According to Timoshenko's beam theory and Allen's sandwich beam theory, the core layer of the structure is a continuous structure, and there is currently no sandwich structure beam composed of discontinuous core layers. Therefore, from the perspective of beam safety, this study defines the equivalent stiffness of pyramid and grid sandwich structure plate members as:

The flexural stiffness of the material itself is calculated as follows,

$$D_{eq} = D_f + D_0 \tag{7}$$

where E is the elastic modulus of the panel (MPa), I is the moment of inertia of the cross-section (mm^4), and l is the flexural length of the cross-section (mm).

The deflection of sandwich structure beams is calculated by Eq. 8,

$$\delta = \frac{Fl^3}{48D_{eq}} \tag{8}$$

where δ is the deflection of sandwich structure beam (mm), and F is the load (N).

In anti-bending structures, energy absorption mainly occurs when the structure is subjected to bending moments, and the structure absorbs and disperses energy through deformation, thereby preventing the structure from being damaged by excessive stress. Energy absorption is the ability of a structure to convert external input energy into internal energy through deformation, fracture, and other processes when subjected to external forces, and store or dissipate it. In sandwich structure plate members, this energy absorption capacity is mainly reflected in the deformation and failure process of the core material.

The equation for the energy absorption characteristic E of the sandwich structural plate members under bending load can be expressed as follows,

$$E = \int_0^{x_{max}} F(x)dx \tag{9}$$

where x_{max} is the maximum displacement during loading (mm), x is the displacement in the loading segment (mm), and $F(x)$ is the corresponding load (N).

Specific Energy Absorption (SEA) is a key indicator for measuring the energy

absorption capacity per unit mass of a structure, reflecting how much energy the structure can absorb per unit mass when subjected to external forces. It mainly evaluates the efficiency of material utilization in the energy absorption process. The SEA equation is the ratio of energy absorption to structural mass. The higher the SEA value, the higher the material utilization efficiency. The statement is as follows,

$$SEA = \frac{\int_0^{x_{max}} f(x)dx}{m} \tag{10}$$

where m denotes the total mass of the structure.

Finite Element Analysis

The deformation behavior of four types of sandwich structural plate members under bending load was analyzed using Auto Inventor software. The geometric parameters of the finite element analysis model were consistent with the actual specimens. The material parameters shown in Table 1 are the same as those simulated by the finite element method.

The simulation process involves fixing the specimens on a bracket made of structural steel and applying a loading head to the panel above it. The lower panel of the specimen model is connected to the bracket in a separated but non sliding manner. Due to the complexity of simulating the elastic-plastic changes of wood-based structural specimens under bending loads, it is difficult to quantitatively describe them. Therefore, this article only qualitatively analyzed the changing state of the specimens under bending loads. The entity unit used was C3D4, and the model contains a total of 114222 nodes and 59965 elements. By analyzing the bearing capacity of four types of specimens of the sandwich structure plate members, their stress distribution was explored under bending loads.

Based on the ultimate stress of core materials (50.28MPa), the flexural ability of four kinds of sandwich structural plate members was analyzed. In the structural design of construction projects, the safety factor is usually used to indicate the degree of safety of the structure. Therefore, the failure state and failure sequence of the structure can be determined from the safety factor. In Fig. 5, the distribution of safety factors for four types of sandwich structure plate members is shown. In the simulation results, the failure of Type I and Type RI structural plate members mainly occurred at the root of the core. Under the same bending load, the bending deformation of Type RI structural plate members was smaller than that of Type I structural plate members, and the reinforcement effect was significant. The failure of Type II and RII structural plate members mainly occurred on the supporting plates on both sides of the applied load. The most dangerous part of the test plate members was concentrated at the contact between the rib plate and the panel groove, and the deformation was also the largest here. When the II-type specimen the most dangerous part of the test plate members is concentrated at the contact between the rib plate and the panel groove, and the deformation was also the largest here. It underwent significant bending deformation, such that both the rib plate and the panel simultaneously bore corresponding bending stress. Under the same flexural load, the stress of RII-type structural plate members is mainly concentrated in the rib plates due to the strengthening effect of the panels. Comparing II-type and I-type structural plate members, the safety factor of II-type structural plate members was significantly higher than that of I-type. This is because the stress distribution of II-type structural plate members is relatively dispersed, and both the panel and rib plates bear the load simultaneously. The core of I-type structural plate members is the main force bearing the flexural load, especially at the root of the core,

bioresources.cnr.ncsu.edu

which needs to bear the combined action of flexural load and shear load. The bending deformation of the core is large, and the safety factor at the root of the core is the lowest.
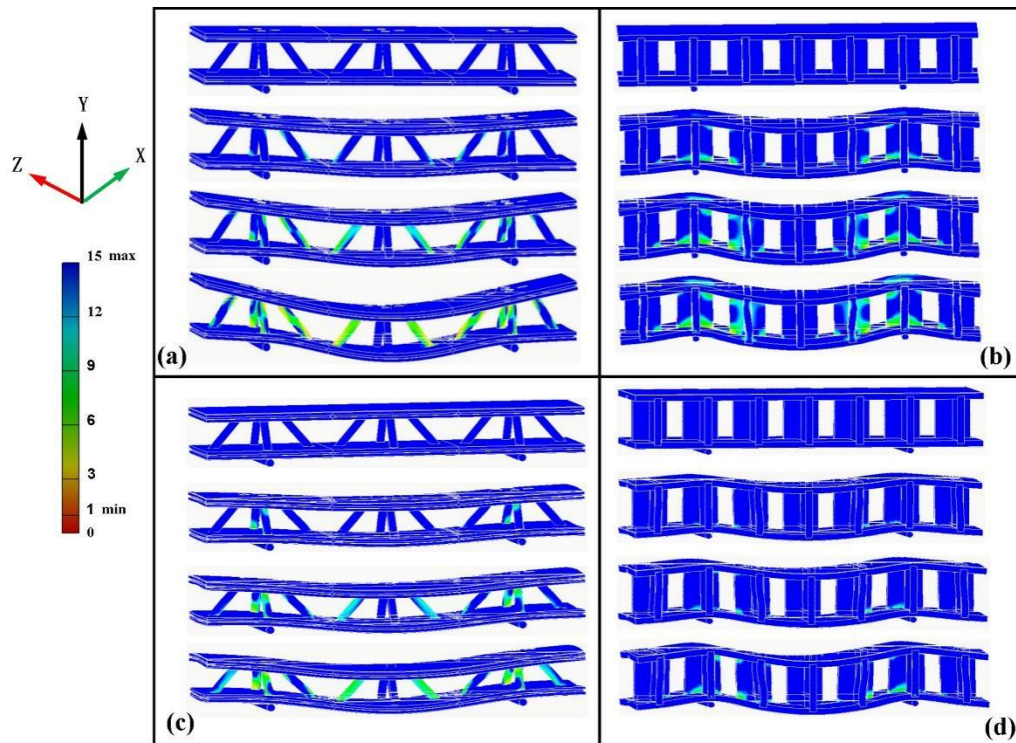

Fig. 5. Safety factor distribution of the simulation structure: (a) I-type structural plate members; (b) II-type structural plate members; (c) RI-type structural plate members; and (d) RII-type structural plate members

RESULTS AND DISCUSSION

Flexural Failure Mode of Specimens

According to ASTM D7249 (2016) and ASTM D7250 (2016), four-point bending tests were conducted on wood-based sandwich structural plate members. The failure mode of the specimen is shown in Fig. 6. The I-type specimen in Fig. 6 is a prefabricated pyramid sandwich structure plate member, the RI-type specimen is a panel reinforced prefabricated pyramid sandwich structure plate member, the II-type specimen is a grid sandwich structure plate member, and the RII-type specimen is a panel reinforced grid sandwich structure plate member. The failure behavior of these four structural plate members under flexural loads mainly manifested as delamination between components, fracture of panel fibers, and buckling failure of the cores. The panel reinforced specimens displayed good structural stability and improved the integrity of the specimens in failure tests.

As shown in Fig. 6, the failure mode of I-type specimen is that the lower panel separates at the cell connection and the upper panel cracks at the cell connection. The failure mode of RI-type specimen is mainly bending deformation of the plate members, bending deformation of the core, and failure at the connection between the core and the panel. The failure mode of II-type specimen is that the entire specimen undergoes bending deformation, and the lower panel fractures at the maximum deflection. The failure mode of RII-type specimen is that the entire specimen undergoes bending deformation, with the

upper panel cracking at the maximum deflection and the rib plate being pulled out of the lower panel groove.

The failure modes of both RI-type and RII-type specimens exhibited significant bending deformation, which is consistent with the simulation results in Fig. 5. The panel of the RII-type specimen was covered with glass fiber, which served as a reinforcing material and was able to effectively disperse and resist flexural loads, reducing local stress concentration in the panel. Due to the reinforcement of the panel, the bending resistance of the specimen was enhanced, resulting in the rib plate being pulled out of the lower panel under significant bending deformation and the specimen being damaged.

The degree of damage to the RI-type and RII-type specimens was not significant because the high modulus characteristics of glass fibers helped maintain the shape stability of the specimen structure and reduce sudden failure under bending loads. Due to the reinforcing effect of glass fiber, the failure process became gradual and exhibited good energy absorption capacity.
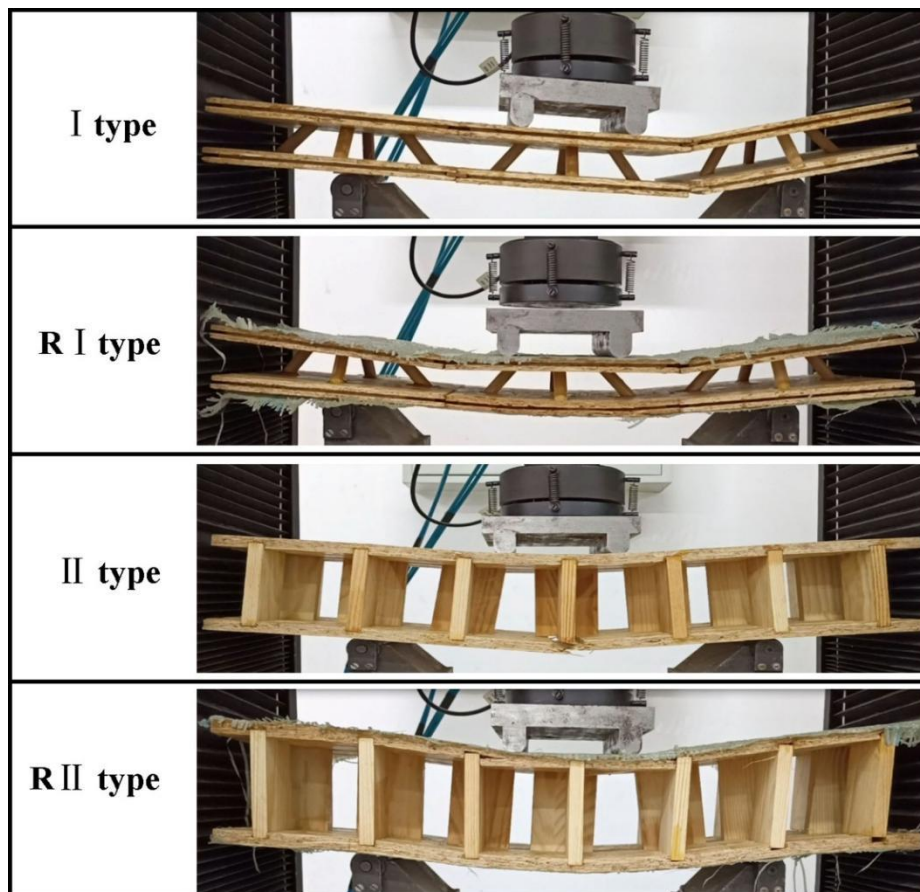

Fig. 6. Failure modes of four specimens

Table 5 shows that there are two phenomena of debonding and core buckling when the four specimens are damaged by force. Core buckling was the main failure mode of the four specimens. The failure mode of delamination of panel did not occur in the I-type specimen because the bonding force between cells was far less than that of panel material. The failure mode of RII type specimen without panel failure was due to the reinforcement effect of GFRC material on the panel.

Table 5. Summary of Failure Modes for the Bending Test

Type	Peak Load (N)		Failure Modes			
	AVG	SD	DLM	DBD	CB	FF
I	1903.44	100.95	0	3	5	5
RI	2637.68	135.63	1	5	5	3
II	3377.60	178.17	3	1	5	5
RII	2499.27	126.53	5	5	1	0

DLM= facesheet delamination; DBD=debonding; CB=core buckling; FF=facesheet failure. Numbers of specimens out five identical specimens with identical failure mode for each orientation angle group.

Flexural Results

The load-deflection curves of wood-based sandwich structural plate members are shown in Fig. 7. From the curves in Fig. 7, it can be observed that during the elastic stage, increasing the bending load linearly increased the displacement of the specimen. The larger the slope of the curve, the greater the bending stiffness of the specimen. As the bending load continued to increase, the specimen entered the inelastic stage, where local deformation or damage occurred. At this point, the increase in relative displacement of the specimen was greater than that in the elastic stage. When there was a significant decrease in bending load, the specimen failed, and the displacement of the specimen continued to increase until it fractured and failed.
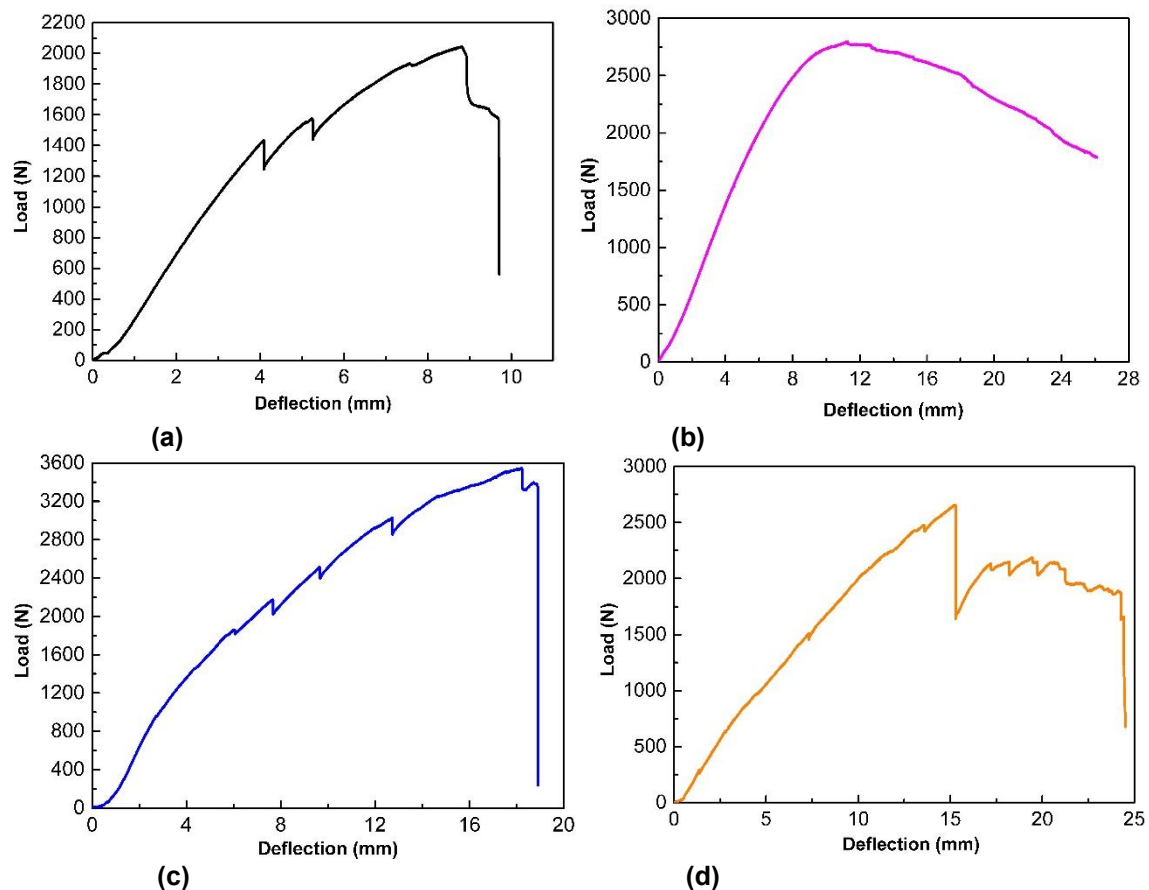

Fig. 7. Load-deflection curves of wood-based sandwich structure plate member in static bending tests. (a) Type Ⅰ specimen; (b) Type Ⅱ specimen; (c) Type R Ⅰ specimen; (d) Type R Ⅱ specimen

From Fig. 7, it can be observed that among the four specimens of these two structural plate members, the II-type specimen bore the highest bending load, while the type I-type specimen bore the smallest bending load. The RI-type specimen had a strengthening effect on the bearing capacity, while the strengthening effect of the RII-type specimen was not significant.

It can be observed from the curve shape in Fig. 7 (a) and (c), both I-type specimens and II-type specimens were in the linear elastic stage at the initial stage of bending load. As the load continued to increase, the curve rose in a sawtooth shape. This can be attributed to the non-uniform deformation in the specimens during the loading process. The interface between the core and the panel will slip, and adhesive failure and the panel and the core will peel off, which will lead to the discontinuity of load transfer. During the continued loading process, mechanical equilibrium will be re-achieved, and this process of destruction and rebalancing will produce sawtooth-shaped fluctuations on the load-deflection curve, resulting in a sawtooth shaped rise on the load-deflection curve. The phenomenon of a linear decrease in the bearing capacity of I-type and II-type specimens after reaching the ultimate load is consistent with the phenomenon of specimen failure. When the specimen reaches its ultimate bending strength, interface separation occurs in I-type specimens, and lower panel fracture occurs in II-type specimen. The overall shape of the specimen structure changes, resulting in structural failure and a sudden decrease in bearing capacity.

The load-deflection curve of the face panel reinforced specimen of the pyramid sandwich structural plate members is shown in Fig. 7 (b). The curve can be roughly divided into three stages: the elastic stage, the yielding stage, and the descending stage after peak load. In the elastic stage, the curve rises sharply and can be approximated as a straight line. It begins to decline after reaching its peak. Compared to the other three types of specimen curves, the load-deflection curve of the RI-type specimen was smoother. This indicates that the RI-type specimen exhibited better homogeneity and consistency during the stress process. The good bonding between OSB and glass fiber reinforced material enabled the specimen to withstand flexural loads uniformly, reducing local stress concentration. The addition of glass fiber effectively dispersed the load evenly and reduced the stress concentration caused by local defects or material inhomogeneity of the specimen. Effectively improved the overall stiffness and strength of the specimens of the wooden based pyramid sandwich structure plate members. The smooth curve also means that when the specimen is subjected to bending loads, there are fewer internal defects in the structure, and fewer cracks, adhesive failure, cracking, and so on. This is consistent with the failure phenomenon of RI-type specimen.

The load-deflection curve of the face panel reinforced specimen of the grid sandwich structure plate members is shown in Fig. 7 (d). The load-deflection curve of the RII-type specimen was shaped as follows: it first rose with a sawtooth shape to reach the maximum load limit. Then it dropped vertically, and finally it fell again through a pulsating wave. This indicates that there was uneven stress distribution inside the specimen structure during the initial stage of flexural load loading. In the state of continuous loading, small slippage and adhesive failure occurred at the joint of the rib plate and the panel in the specimen, resulting in zigzag fluctuations in the force-deflection curve. At this time, the reinforcement effect of the glass fiber had not been brought into play. When the load-deflection curve reached the limit load, the vertical drop was due to the stratification of the upper panel of the specimen, resulting in a sudden decline in the bearing capacity of the specimen. After that, the load-deflection curve exhibited a pulse fluctuation, which means

that the rib plate in the specimen was adhesive failure and separating from the lower panel in turn, but the specimen still retained a certain bearing capacity. At this point, the structure was already in an unstable state. Fluctuations were caused by the redistribution of internal stresses in residual structures under flexural loads.

Table 6. The Mechanical Properties of Four Test Specimens

Name	Secant Stiffness (N/Mm)				Tangent Stiffness (N·Mm)				Ductility (%)			
	I	R I	II	R II	I	R I	II	R II	I	R I	II	R II
0.1Fmax	240.00	255.96	243.49	191.12	390.25	307.38	341.63	195.13	0.0004	0.0007	0.0012	0.0011
0.2Fmax	307.22	296.03	330.00	222.80	409.70	352.11	409.76	273.12	0.0010	0.0020	0.0026	0.0032
0.3Fmax	338.12	322.50	347.39	225.00	438.87	409.84	511.97	307.25	0.0018	0.0038	0.0052	0.0070
0.4Fmax	353.90	336.04	336.97	211.13	468.09	469.20	614.50	351.12	0.0030	0.0062	0.0099	0.0141
Fmax	232.42	248.67	194.73	174.20	117.13	291.10	307.38	115.45	0.0430	0.0703	0.1841	0.1291

Secant stiffness is the slope of the line between a point on the force displacement curve and the origin. Secant stiffness can be used to evaluate the stiffness characteristics of structural materials under different degrees of deformation, and then to evaluate the mechanical properties of structures. Tangent stiffness is the tangent slope of a point on the force displacement curve. The tangent stiffness reflects the local stiffness of the structural material under the current displacement. It is suitable for describing the characteristics of the structural material in the elastic or small deformation stage. Ductility is the ability of a structure to withstand plastic deformation before fracture. Common ductility indexes include elongation and reduction of area. The panel of the specimen of the sandwich structure plate members in this experiment is not completely damaged, so it is difficult to measure the reduction of area, so the elongation of the specimen is used to calculate the ductility. The elongation of the test specimen is calculated as the ratio of the elongation of the test specimen after stress to the original length of the test specimen.

The secant stiffness and tangent stiffness of the four specimens increased with the increase of load between 0.1 and 0.4 of the maximum force. When the load reached the maximum value, the secant stiffness and tangent stiffness both reached the minimum value. This shows that the four types of specimens were in the elastic stage at the initial stage of loading, and the specimens displayed good resistance to external load and show high stiffness. With the continuous increase of load, due to the characteristics of structural materials and the influence of connecting interface and other factors, the structure will gradually enter the stage of nonlinear deformation. When the peak load is reached, the structure will absorb more energy, local damage and structural instability, thus reducing the structural stiffness. The ductility of the four types of specimens increased with the increase of load. When the load was the maximum, the ductility of the specimens was also the maximum. The results show that the specimen of the sandwich structure plate members had good plasticity under large load, such that they were able to withstand large deformation and had good energy absorption capacity. Due to the fact that wood is an anisotropic material, with the continuous increase of load, cracks, bending, delamination and rib pulling out from the panel may begin to appear in the structure, which will also increase the ductility of the structure. In these three indicators, the value of II-type specimen was the largest, and II-type specimen had the best performance in these four types of specimens.

The load-deflection curve shown in Fig. 7 is the load-mid span deflection curve of the specimen. In the bending test of the specimen, only the mid-span displacement of the specimen was measured, and the displacement at the support was ignored. This may result in an initial softening phenomenon in the load-displacement response. Initial softening refers to the phenomenon where, in the initial stage of the load displacement curve, as the load increases, the rate of displacement increase is relatively fast, resulting in a "softening" trend in the curve at this stage. This softening leads to nonlinearity between load and displacement.

Due to factors such as the core structure form, the connection strength between panels and core layers, the unevenness of raw materials, and the gap between the loading system of the testing device and the specimen at the beginning of the test, wooden based sandwich panel members may experience local deformation during the initial loading stage, resulting in an initial softening trend on the load displacement curve. At the initial loading stage of specimen testing, there will not be an immediate linear stress-strain relationship.

In future experiments, methods such as optimizing the bonding between sandwich structure materials and panels, calibrating the loading system, and improving the installation accuracy of specimens can be used to reduce the impact of initial softening phenomenon on the experimental results of wood-based sandwich structure panel components.

Flexural Performance of Sandwich Structure Plate Members

Flexural performance tests were conducted on the four types of the specimens of the sandwich structure plate members, comparing and analyzing their mechanical properties. I-type is represented by a line at a 45 ° angle to the horizontal direction, RI-type is represented by a grid form, II-type is represented by vertical lines, and RII-type is represented by horizontal lines.
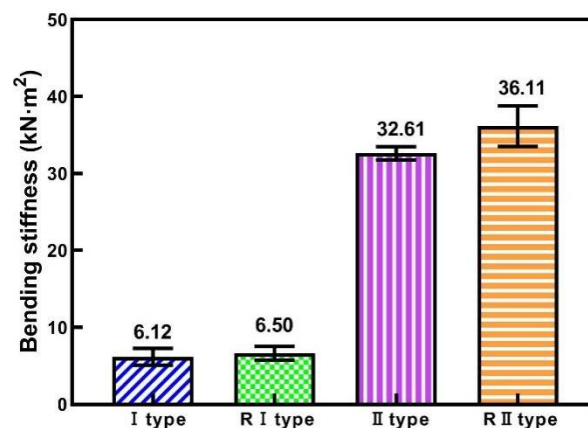

Fig. 8. The bending stiffness of four sandwich structure plate members

Bending stiffness is one of the important performance indicators of the rigidity of sandwich structure plate members. The bending stiffness directly reflects the ability of sandwich structural plate members to resist deformation under bending loads. The higher the stiffness, the smaller the bending deformation of the plate members under the same load. Figure 8 shows the bending stiffness of these four sandwich structure plate members. The bending stiffness of RII-type specimens was the highest, while that of I-type specimens

was the lowest. Compared with specimens of the same type, the bending stiffness of RI specimens was 6.21% higher than that of I specimens, and the bending stiffness of RII specimens was 10.73% higher than that of II specimens. The bonding of a layer of GFRC on the panel had a positive effect on enhancing the flexural stiffness of sandwich structural plate members.

The bending stiffness of II-type specimens was 5.33 times that of I-type specimens, and the bending stiffness of RII-type specimens was 5.55 times that of RI-type specimens. The main reason for the significant difference in bending stiffness between these two sandwich structure plate members is the different structural types of the core layer. The core layer of the grid sandwich structure plate members is composed of many rib plates with multiple support points, which can effectively transmit shear and bending moments. This structural form helps to disperse external loads, reduce local deformation, and thus improve the overall bending stiffness of sandwich structural plate members. The core structure of the pyramid shaped sandwich structure plate members is similar to the truss structure. Under external loads, the core undergoes significant bending deformation, and the danger point of the structure appears at the root of the core, resulting in a decrease in overall stiffness.

Figure 9 shows the bending stiffness of sandwich plate members with different core structure types. The horizontal axis in Fig. 9 represents relative density (the relative density of sandwich structure plate members is the ratio of the density of the cores to the solid material density of the sandwich structure plate members cells).
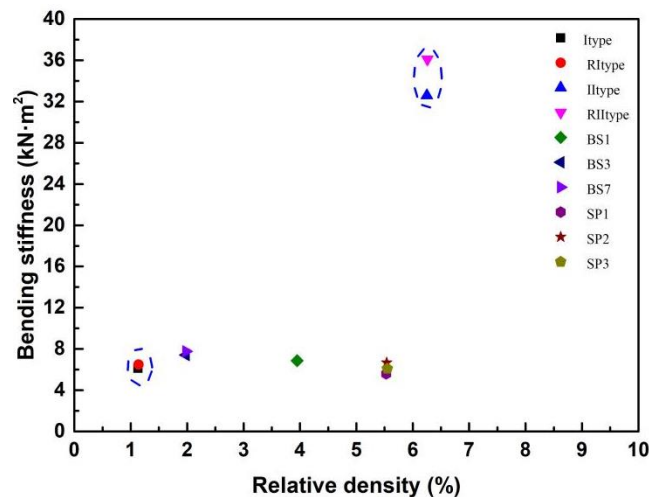

Fig. 9. Bending stiffness of sandwich structures with different core structure forms

Zheng and Li *et al.* researchers refer to this type of long sandwich structure as a beam. BS1, BS3, and BS7 are X-typed core sandwich structure beam specimens studied by Zheng *et al.* (2021). The raw materials for sandwich structure beam specimens were OSB and birch. Based on the diameter of the core, the angle between the core and the panel, and the different depths of the core in the panel, multiple specimens were constructed and subjected to bending stiffness analysis. SP1, SP2, and SP3 were sandwich beam specimens with a bi-directional grids structure core structure studied by Li *et al.* (2016). The sandwich structure beam specimens were prepared from phenolic impregnated laminated paper (NP610) with the nominal thickness of 2.4 mm. These experimental results are compared in Fig. 9 with the bending stiffness of the specimens in this study. It is apparent that an

increase in the relative density of the sandwich structure beam can improve the bending stiffness to a certain extent. The mechanical properties of the core material, the connection method between the core material and the panel, and the geometric configuration of the core layer all will have an impact on the bending stiffness of sandwich structural beams.

Table 7 lists the deflection of four sandwich structure plate members under maximum bending load, and the results show that the experimental values were higher than the theoretical calculation values, and the simulation values were higher than the experimental values. This result is consistent with the research findings of Zheng *et al*. (2021). The deflection calculation of the four sandwich structure plate members in this study is based on Eq. 10. In theoretical calculations, it is assumed that the shear deformation of sandwich beams can be ignored. At present, there is no unified deflection formula that can directly calculate the sandwich structure beam with a periodic core structure. Therefore, this theoretical calculation is based on the general principles of mechanics to derive a rough calculation. Under bending loads, sandwich structure beams experience tensile and compressive stresses on the panels, while the core layer mainly experiences shear stress. The interaction between the shear deformation of the core layer and the bending deformation of the panel has a significant impact on the deflection. This complex stress distribution is the main reason for the experimental deflection values being greater than the theoretical calculated values.

The simulation value was higher than the experimental value. Although the material parameters used in the simulation were the same as those in the experiment, there was a gap between the simulation and the actual material during the simulation. The real-time changes of the actual material under the action of bending load cannot be represented. In the simulation, friction and clearance between sandwich structure plate members and bearing and load are ignored. These factors affect the experimental results.

Table 7. Experimental and Theoretical Values of Deflection of the Four Sandwich Structure Plate Members

Type	Height of the specimen (mm)	Fmax (N)	Experimental values (mm)	Theoretical values (mm)	Simulation value(mm)
I	52	2043.78	8.79	1.50	11.23
RI	53	2769.23	11.25	1.92	12.75
II	106	3546.47	18.21	0.50	22.36
RII	107	2656.24	15.247	0.36	19.41
* The numbers in the table represent the mean ± standard deviation; The application of one-way ANOVA showed significant differences ($p < 0.001$).					

For bending-resistant structures, when subjected to load and undergoing bending, the structure absorbs a portion of energy to change its shape. This energy absorption performance is crucial for the safety and durability of the structure. Figure 10 shows the energy absorption characteristics of the specimens of the four sandwich structure plate members. According to the Load-deflection curves shown in Fig. 7, when the bending load of the I-type specimen reached its maximum value, it absorbed 9.67 J of energy, accounting for 87.67% of the total energy of the specimen. When the bending load of the RI-type specimen reached its maximum value, it absorbed 4.94 J of energy, accounting for 25.57% of the total energy of the specimen. When the bending load of the II-type specimen reached its maximum value, it absorbed 38.03 J of energy, accounting for 94.44% of the total energy of the specimen. When the bending load of the RII-type specimen reached its

maximum value, it absorbed 12.29 J of energy, accounting for 54.57% of the total energy of the specimen. This result indicates that the panel-reinforced sandwich structure plate members had the ability to undergo stable plastic deformation and improve energy absorption after being damaged.

The energy absorption performance of the grid sandwich structure plate members was higher than that of the pyramid sandwich structure plate members. This is because the core layer of the grid sandwich structure plate members was composed of a series of rib plates, and the panel connected all rib plates into one. This structural form can effectively disperse and transfer loads when subjected to external forces, thereby increasing the overall stability and energy absorption capacity of the structure. The pyramid sandwich structure plate members is composed of individual cells spliced together and connected. Although it also has a certain load-bearing capacity, its geometric configuration limits the uniform distribution and transmission efficiency of the load. This phenomenon can be observed from the stress distribution in the simulation diagram of Fig. 5. When subjected to bending loads, the displacement in the load-deflection curve of the grid sandwich structure plate members is relatively long, which is a direct reflection of the continuous energy absorption of the structure during the failure process. The displacement in the load-deflection curve of the pyramid type sandwich structure plate members is relatively short, resulting in relatively poor energy absorption performance.
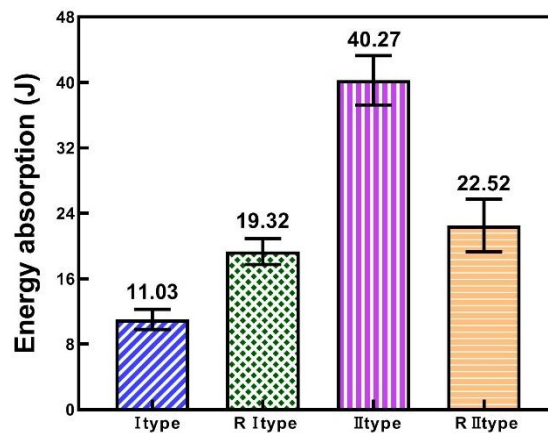

Fig. 10. The energy absorption of four sandwich structure plate members

Specific energy absorption (SEA) is the energy absorbed by a unit mass of material during the failure process. It is an important indicator for measuring the energy absorption efficiency of structural plate members. By comparing the SEA values of different sandwich structure plate members, the energy absorption performance of sandwich structure plate members can be intuitively reflected. The higher the SEA ratio, the more energy the structure can absorb under the same mass, usually indicating better impact or seismic resistance (Zhang *et al*. 2020).

Figure 11 shows the SEA characteristics of four sandwich structure plate members specimens. The SEA value of II-type specimen was the highest, while that of I-type specimen was the lowest. Compared with similar structures, the SEA value of II-type specimen was 79.62% higher than that of RII-type specimen. The SEA value of the RI-type specimen was 68.92% higher than that of the I-type specimen. The RI-type specimen was 15.95% higher than the RII-type specimen.

The II-type grid sandwich structure plate members is composed of multiple rib plates in the core layer structure. This structure has good spatial stability and porosity, and it can provide more energy absorption paths under flexural loads, so that energy is more evenly distributed throughout the structure. At the same time, it triggers multi-stage progressive structural failure, thereby absorbing more energy and helping to improve the SEA. This characteristic can be demonstrated from Fig. 7 (c). The panel of RII-type grid sandwich structure plate members was laid with glass fiber, which increased the stiffness and strength of the panel, resulting in brittle fracture rather than plastic deformation during the failure process, thereby reducing the SEA. This characteristic can be demonstrated from Fig. 7 (d).

The SEA of pyramid shaped sandwich structure plate members was lower than that of grid shaped sandwich structure plate members, due to the geometric configuration of the core layer limiting the uniform distribution and transmission efficiency of the load, resulting in relatively weak energy absorption capacity. The SEA of RI-type specimen was higher than that of I-type specimen, and the reinforcement of the panel plays a significant role.
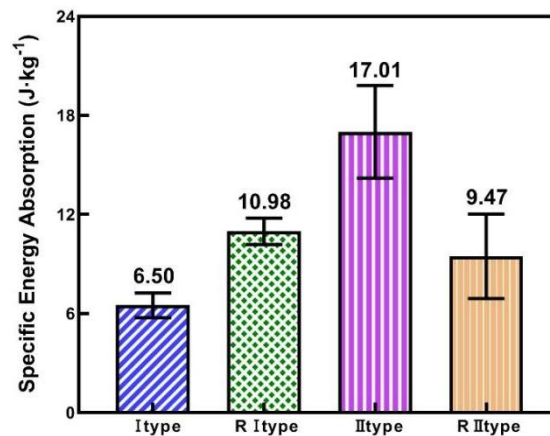

Fig. 11. The specific energy absorption of four sandwich structure plate members

The type II specimen exhibited better performance than the RII-type specimen in energy absorption and specific energy absorption, which can be attributed to the large bearing capacity of type II specimen. From the simulation results shown in Fig. 5 for the test specimens subjected to bending load, it can be observed that the failure of the RII specimen mainly occurred at the contact positions between the ribs and the lower plate. These positions are all located in the support area of the lower plate. These failure positions are consistent with the experimental failure locations shown in Fig. 6. The RII-type specimen not only enhanced the performance of the panel, but it also changed the relative stiffness ratio of the panel and the core material, resulting in the failure of the core material to give full play to its bearing capacity under bending load, weakening the interaction between the panel and the core, and thus reducing the bearing capacity of the specimen. In the four point bending test, the panel reinforced structure changed the load distribution ratio between the panel and the core. At the same time, it also changed the transmission path and efficiency of stress between the panel and the core, so that more loads are borne by the panel, and the bearing capacity of the panel was greater than the bonding strength between the rib and the panel, resulting in the rib becoming pulled out from the lower panel, the specimen being damaged, and the bearing capacity becoming decreased.

CONCLUSIONS

1. The flexural test showed that the transmission path and efficiency between the panels and the core layer of the specimen had a decisive impact on the bending-resistance performance of the specimen. The core layer of the pyramid sandwich structure plate members was composed of multiple pyramid cells, which allowed most of the load to be transmitted through the cells and reduced the direct stress on the panel. As the load continued to increase, damage occurred at the weak links of the structure, and eventually the lower panel cracked at the connection between the cells. The core layer of the grid type sandwich structure plate members was composed of a series of parallel rib plates, and the load transmission path is the interaction between the panels and the rib plates. At the maximum displacement of the lower panel, it was not only subjected to flexural stress, but also to local shear stress caused by deformation of the panels and rib plates, resulting in material failure at that location.

2. The core layer configuration determined the relative stiffness ratio between the panels and the core layer, resulting in the reinforcement of the panel not necessarily effectively enhancing the overall bending-resistance performance of the specimen. The interaction between the panels and core layer of the RI-type pyramid sandwich structure plate members was enhanced, and the flexural performance of the specimen was improved, while the interaction between the panels and core layer of the RII-type grid sandwich structure plate members was weakened, reducing the flexural performance of the specimen.

3. For sandwich structures plate members of the same type, plate reinforcement can improve the bending stiffness of the specimen and enhance its bending resistance. After being damaged, the specimen has the ability to stabilize plastic deformation and improve energy absorption.

ACKNOWLEDGMENTS

REFERENCES CITED

Allen, H. G. (1969). "The structure of cellular solids," in: *Analysis and Design of Structural Sandwich Panels*, Pergamon Press, London. DOI: 10.1016/B978-0-08-012870-2.50006-7

Almutairi, A. D., Bai, Y., and Ferdous, W. (2023). "Flexural behaviour of GFRP-softwood sandwich panels for prefabricated building construction," *Polymers* 15(9), 1-21. DOI: 10.3390/polym 15092102

Amir, A. L., Ishak, M. R., Yidris, N., Zuhri, M. Y. M., Asyraf, M. R. M., and Zakaria, S. Z. S. (2023). "Influence of woven glass-fibre pre-preg orientation on the flexural properties of a sustainable composite honeycomb sandwich panel for structural applications," *Materials* 16(14), 1-17. DOI: 10. 3390/ma16145021

Amir, A. L., Ishak, M. R., Yidris, N., Zuhri, M. Y. M., and Asyraf, M. R. M. (2021). "Potential of honeycomb-filled composite structure in composite cross-arm component: A review on recent progress and its mechanical properties," *Polymers* 13(8), 1-24. DOI: 10.3390/polym13081341

Ardalany, M., Fragiacomo, M., Carradine, D., and Moss, P. (2013). "Experimental behavior of laminated veneer lumber (LVL) joists with holes and different methods of reinforcement," *Engineering Structures* 56(8), 2154-2164. DOI: 10.1016/j.engstruct.2013.08.034

ASTM C393 M-06 (2006). "Standard test method for core shear properties of sandwich constructions by beam flexure," ASTM International, West Conshohocken, PA, USA.

ASTM D7249M-16 (2016). "Standard test method for facing properties of sandwich constructions by long beam flexure," ASTM International, West Conshohocken, PA, USA.

ASTM D7250M-16 (2016). "Standard practice for determining sandwich beam flexural and shear stiffness," ASTM International, West Conshohocken, PA, USA.

Aydin, R., Yuksel, E., Yardimci, N., and Gokce, T. (2016). "Cyclic behaviour of diagonally stiffened beam to column connections of corrugated web I sections," *Engineering Structures* 121(8), 120-135. DOI: 10.1016/j.engstruct.2016.04.036

Blanco, D., Rubio, E. M., Lorente-Pedreille, R. M., and Sáenz-Nuño, M. A. (2021). "Lightweight structural materials in open access: Latest trends," *Materials* 14(1), 1-28. DOI: 10.3390/ma14216577

Chen, G., Tan, C., Yang, W. Q., Wu, J., Zhou, T., Jiang, H., and Zhang, Y. (2021). "Wood I-joists with web holes and flange notches: A literature review," *Journal of Building Engineering* 38(6), 1-12. DOI: 10.1016/j.jobe.2021.102224

De Santis, Y., Pasquale, D., Aloisio, A., Stenstad, A., and Mahnert, K. C. (2023). "Experimental, analytical, and numerical investigation on the capacity of composite glulam beams with holes," *Engineering Structures* 285(6), 989-1037. DOI: 10.1016/j.engstruct.2023.115995

Dubina, D., Ungureanu, V., and Gilia, L. (2015). "Experimental investigations of cold formed steel beams of corrugated web and built-up section for flanges," *Thin Walled Structures* 90(5), 159-170. DOI: 10.1016/j.tws.2015.01.018

Du, B., Liu, H.-C., Pan, X., Qin, W.-M., and Chen, L.-M. (2022). "Progress in fusion bonding of thermoplastic composite sandwich structures," *Acta Materiae Compositae Sinica* 39(07), 3044-3058. DOI: 10.13801/j.cnki.fhclxb.20220228.001

Faidzi, M. K., Abdullah, S., Abdullah, M. F., Azman, A. H., Hui, D., and Singh, S. S. K. (2021). "Review of current trends for metal-based sandwich panel: Failure mechanisms and their contribution factors," *Engineering Failure Analysis* 123(5), 302-310. DOI: 10.1016/j.engfailanal.2021.105302

Feng, W. (2008). *Predicting Coefficient of Thermal Expansion and Designing Optimum Structure of Sandwich Construction Composites*, Master's Thesis, Harbin Institute of Technology, Harbin, China. DOI: 10.7666/d.D271716

Han, B., Zhang, Z. J., Zhang, Q. C., Zhang, Q., Lu, T. J., and Lu, B. H. (2017). "Recent advances in hybrid lattice-cored sandwiches for enhanced multifunctional performance," *Extreme Mechanics Letters* 10(1), 58-69. DOI: 10.1016/j.eml.2016.11.009

Hao, J. X., Wu, X. F., Oporto, G., Wang, J. X., Dahle, G., and Nan, N. (2018). "Deformation and failure behavior of wooden sandwich composites with Taiji honeycomb core under a three point bending test," *Materials* 11(11), 567-575. DOI:

10.3390/ma11112325

Hara, D., and Ozgen, G. O. (2016). "Investigation of weight reduction of automotive body structures with the use of sandwich materials," *Transportation Research Procedia* 14, 1013-1020. DOI: 10.1016/j.trpro.2016.05.081

Hassan, H. Z., and Saeed, N. M. (2024). "Advancements and applications of light weight structures: A comprehensive review," *Discover Civil Engineering* 1(8), 1-43. DOI: 10.1007/s44290-024-00049-z

Huang, R., Mao, H., Kim, B., and Wu, Q. (2014). "Flexural and thermal expansion properties of core shell structure wood polymer composites," *Journal of Zhejiang Forestry Science and Technology* 34(06), 40-44. DOI: 10.3969/j.issn.1001-3776.2014.06.009

Jiao, P. C., Borchani, W., Soleimani, S., and McGraw, B. (2017). "Lateral-torsional buck ling analysis of wood composite I-beams with sinusoidal corrugated web," *Thin Walled Structures* 119(8), 72-82. DOI: 10.1016/j.tws.2017.05.025

Jiloul, A., Blanchet, P., Boudaud, C., and Perez, C. (2024). "Structural evaluation of I-joists with corrugated panel web," *Construction and Building Materials* 442(9), 1-22. DOI: 10.1016/j.conbuildmat.2024.137655

Kamble, Z., Mishra, R. K., Behera, B. K., Tichy, M., Kolar, V., and Muller, M. (2021). "Design, development, and characterization of advanced textile structural hollow composites," *Polymers* 13(2), 1-22. DOI: 10.3390/polym13203535

Kawasaki, T., Zhang, M., and Wan, Q, Komatsu, K., and Kawai, S. (2006). "Elastic moduli and stiffness optimization in four-point bending of wood-based sandwich panel for use as structural insulated walls and floors," *Journal of Wood Science* 52(8), 302-310. DOI: 10.1017/s10086-005-0766-z

Li, J. H., Hunt, J. F., Gong, S. Q., and Cai, Z. Y. (2016). "Fatigue behavior of wood-fiber-based tri-axial engineered sandwich composite panels (ESCP)," *Holzforschung* 70(6), 567-575. DOI: 10.1515/hf-2015-0091

Li, K., Li, J., Tang, Q., and Wang, Y. (2024). "Research on the mechanical behavior of GFRP reinforced glulam beam column glued rod joints," *Journal of Qingdao University of Technology* 45(3), 11-18. DOI: 10.3969/j.issn.1673-4602.2024.03.002

Lukawski, D., Hochmanska Kaniewska, P., Janiszewska Latterini, D., and Lekawa Raus, A. (2023). "Functional materials based on wood, carbon nanotubes and graphene: Manufacturing, applications, and green perspectives," *Wood Science and Technology* 57(8), 989-1037. DOI: 10.1007/s00226-023-01484-4

Mohammadabadi, M., Miller, J., Street, J., Kim, Y., and Ragon, K. (2023). "Wood based corrugated core sandwich panels manufactured using a wooden mold," *BioResources* 18(2), 3033-3043. DOI: 10.15376/biores.18.2.3033-3043

Pelinski, K., and Smardzewski, J. (2020). "Bending behavior of lightweight wood based sandwich beams with auxetic cellular core," *Polymers* 12(8), 1-15. DOI: 10.3390/polym12081723

Pierre, J., Iervolino, F., Farahani, R. D., Piccirelli, N., Levesque, M., and Therriault, D. (2023). "Material extrusion additive manufacturing of multifunctional sandwich panels with load bearing and acoustic capabilities for aerospace applications," *Additive Manufacturing* 61(5), 1-10. DOI: 10.1016/j.addma.2022.103344

Shi, H., Liu W., Fang H., and Huo R. (2018). "Experimental research on flexural fatigue behavior of GFRP-Balsa sandwich beams," *Acta Materiae Compositae Sinica* 35(05), 1114-1122. DOI: 10.13801/j.cnki.fhclxb.20170707.001

Singh, P., Sheikh, J., and Behera, B. K. (2024). "Metal-faced sandwich composite panels:

A review," *Journal of Wood Science* 195(2), 302-310. DOI:
    10.1016/j.tws.2023.111376

Slonina, M., Dziurka, D., and Smardzewski, J. (2023). "Failure mechanism map for
    bending wood based honeycomb sandwich beams with starch impregnated core,"
    Composite Structures 310(4), 1-11. DOI: 10.1016/j.compstruct.2023.116749

Smardzewski, J., Majnusz, M., and Murlak, K. (2022). "Bending and energy absorption
    performance of novel openwork wooden panels," *European Journal of Wood
    Products* 80(10), 515-528. DOI: 10.1007/s00107-022-01795-6

Tian, C., Tian, Z., Tu, P., Cao, X., Dong, S., and Li, J. (2024). "Research on the energy
    absorption characteristics of lattice composite sandwich structural beams subjected to
    pure bending loads," *Structures* 65(7), 1-13. DOI: 10.1016/j.istruc.2024.106715

Wang, Y. R., Liu, J. M., Jia, L. X., and Chen, Z. H. (2022). "Recent advances in woven
    spacer fabric sandwich composite panels: A review," *Polymers* 14(17), 1-19. DOI:
    10.3390/polym14173537

Wang, Z., Zhou, L., Zhang, Z., and Mwambala, A. M. (2024). "Study on bending
    performance of laminated bamboo sandwich panels with different lattice core layers:
    Cleaner production of green material," *Case Studies in Construction Materials* 20(7),
    1-13. DOI: 10.1016/j.cscm.2024.e03379

Yang, D., Fan, C., and Hu, Y. (2021). "Optimization and mechanical properties of
    fabricated 2D wood pyramid lattice sandwich structures," *Forests* 12(5), 1-17. DOI:
    10.3390/f12050607

Yang, D. X., and Fan, C. S. (2022). "The mechanical properties of wood based grid
    sandwich structures," *Forests* 13(6), 1-22. DOI: 10.3390/f13060877

Zhang, J. Y., Lu, B. Q., Zheng, D. F., and Li, Z. Y. (2020). "Experimental and numerical
    study on energy absorption performance of CFRP/aluminum hybrid square tubes
    under axial loading," *Thin-Walled Structures* 155(8), 1-19. DOI:
    10.1016/j.tws.2020.106948

Zheng, T., Zou, L., and Hu, Y. (2021). "Short beam shear properties and failure modes of
    the wood-based X-type lattice sandwich structure," *Journal of Forestry Research*
    32(2), 877-887. DOI: 10.1007/s11676-020-01137-3

Zulueta, K., Burgoa, A., Lekube, B., Vilas, J. L., and Arrillaga, A. (2022). "Improvement
    of structural vibration damping performance of SMCs through SMC/TPE sandwich
    structures," *Journal of Applied Polymer Science* 139(42), 1-13. DOI:
    10.1002/app.53026